

Open camera or QR reader and  
scan code to access this article  
and other resources online.



# Development of a Self-Assembled Dermal Substitute from Human Fibroblasts Using Long-term Three-Dimensional Culture

Takashi Nakano, MD,<sup>1</sup> Hiroki Yamanaka, MD, PhD,<sup>1,2</sup> Michiharu Sakamoto, MD, PhD,<sup>1</sup>  
Itaru Tsuge, MD, PhD,<sup>1</sup> Yasuhiro Katayama, MD, PhD,<sup>1</sup> Susumu Saito, MD, PhD,<sup>1</sup> Jiro Ono, BA,<sup>3</sup>  
Tetsuji Yamaoka, PhD,<sup>2</sup> and Naoki Morimoto, MD, PhD<sup>1</sup>

Skin substitutes have emerged as an alternative to autografts for the treatment of skin defects. Among them, scaffold-based dermal substitutes have been extensively studied; however, they have certain limitations, such as delayed vascularization, limited elasticity, and the inability to achieve permanent engraftment. Self-assembled, cell-based dermal substitutes are a promising alternative that may overcome these shortcomings but have not yet been developed. In this study, we successfully developed a cell-based dermal substitute (cultured dermis) through the long-term culture of human dermal fibroblasts using the net-mold method, which enables three-dimensional cell culture without the use of a scaffold. Spheroids prepared from human dermal fibroblasts were poured into a net-shaped mold and cultured for 2, 4, or 6 months. The dry weight, tensile strength, collagen and glycosaminoglycan levels, and cell proliferation capacity were assessed and compared among the 2-, 4-, and 6-month culture periods. We found that collagen and glycosaminoglycan levels decreased over time, while the dry weight remained unchanged. Tensile strength increased at 4 months, suggesting that remodeling had progressed. In addition, the cell proliferation capacity was maintained, even after a 6-month culture period. Unexpectedly, the internal part of the cultured dermis became fragile, resulting in the division of the cultured dermis into two collagen-rich tissues, each of which had a thickness of 400  $\mu\text{m}$  and sufficient strength to be sutured during *in vivo* analysis. The divided 4-month cultured dermis was transplanted to skin defects of immunocompromised mice and its wound healing effects were compared to those of a clinically available collagen-based artificial dermis. The cultured dermis promoted epithelialization and angiogenesis more effectively than the collagen-based artificial dermis. Although further improvements are needed, such as the shortening of the culture period and increasing the size of the cultured dermis, we believe that the cultured dermis presented in this study has the potential to be an innovative material for permanent skin coverage.

**Keywords:** dermal substitute, long-term 3D culture, skin substitute, regenerative therapy, scaffold-free, cultured dermis

<sup>1</sup>Department of Plastic and Reconstructive Surgery, Graduate School of Medicine, Kyoto University, Kyoto, Japan.

<sup>2</sup>National Cerebral and Cardiovascular Center Research Institute, Suita, Japan.

<sup>3</sup>Tissue By Net Corporation, Saitama, Japan.

## Impact Statement

This is the first report of the successful development of a self-assembled, cell-based dermal substitute derived from human dermal fibroblasts through long-term three-dimensional culture. The scaffold-free cultured dermis exhibited superior properties, such as sufficient tensile strength, high biocompatibility, and efficacy in promoting wound healing when compared to the collagen-based artificial dermis.

## Introduction

SKIN IS THE largest organ in the human body and plays a crucial role in protection against microorganisms, regulation of body temperature, and detection of sensory information from the external environment.<sup>1</sup> Autologous skin grafts have been widely utilized to treat large skin defects resulting from various causes, including acute trauma, surgical resection of tumors, and chronic diseases<sup>2</sup>; however, autografts have limitations such as donor site morbidities and limited sources. Therefore, significant efforts have been devoted to developing possible alternatives.<sup>3</sup>

As a clinically available skin substitute, cultured epithelial autografts have been established for epidermal regeneration,<sup>4</sup> while various types of bioartificial scaffolds have been used worldwide for dermal tissue regeneration.<sup>5,6</sup> Among them, collagen-based dermal substitutes continue to be extensively studied and provide beneficial results in wound healing.<sup>7,8</sup> For example, animal-derived collagen-based artificial dermis, such as Integra<sup>®</sup> and Pelnac<sup>®</sup>, serve as scaffolds for the ingrowth of fibroblasts and endothelial cells, promoting wound healing.<sup>6,9</sup> However, the remodeling of collagen and promotion of neovascularization presents significant obstacles in scaffold-based dermal regeneration, as the artificial dermis typically requires several weeks to become fully vascularized. This delay in vascularization can lead to the accumulation of fluids and an increased risk of infection.<sup>10–12</sup> In addition, collagen-based dermal substitutes may have limited elasticity, which cannot prevent wound contraction during repair.<sup>13–15</sup> To date, an ideal, fully functional dermal substitute has not yet been developed.<sup>16–19</sup>

To overcome these challenges, researchers have explored alternative approaches to scaffold-based dermal regeneration. One promising approach is the development of a self-assembled, cell-based dermal substitute from human fibroblasts using three-dimensional (3D) culture.<sup>20,21</sup> In 2021, a novel tissue engineering method using a net metal mold, which allows the scaffold-free culture of 3D tissues of unprecedented thickness, was reported by Sakaguchi et al.<sup>22</sup> This method involves assembling spheroids without the use of a scaffold, densely packing them in a net-shaped mold, and shake-culturing them to facilitate cell adherence and formation of 3D tissue. We hypothesized that if 3D tissue derived from dermal fibroblasts is created using a net mold and cultured for a longer period, remodeling of the extracellular matrix (ECM) will progress, resulting in the development of a dermal substitute (called cultured dermis) with greater tensile strength and excellent cytocompatibility.

To test this hypothesis, we performed long-term culture of dermal fibroblasts using the net-mold method for 2, 4, and 6 months, and successfully created a self-assembled cultured dermis. The dry weight, tensile strength, collagen quantification, sulfated glycosaminoglycans (sGAG) quantification,

and cell proliferative capacity of the cultured dermis were evaluated *in vitro*. In addition, we applied a 4-month cultured dermis to skin defects in immunocompromised mice and evaluated the wound healing effects of the cultured dermis compared with a clinically available collagen-based artificial dermis.

## Materials and Methods

### Ethical approval

The animal study was conducted at Kyoto University following the Guidelines for Animal Experimentation of Kyoto University, Japan. The protocol was approved by the Animal Research Committee of the Kyoto University Graduate School of Medicine (permit number: Med Kyo 20515), and the number of experimental animals used was kept to a minimum.

### Preparation of cultured dermis

**Cell culture.** Normal human dermal neonatal fibroblasts (NHDF; CC-2509; Lonza, Basel, Switzerland) were cultured in serum-free medium for human fibroblast (FKCM; Fukoku, Saitama, Japan) supplemented with 10% fetal bovine serum (FBS; Gibco, Thermo Fisher Scientific, Waltham, MA) and 1% penicillin-streptomycin (Sigma-Aldrich, St. Louis, MO), and incubated at 37°C and 5% carbon dioxide (CO<sub>2</sub>) for 3 days until the next passage. The cells were expanded and used at passages 4–5.

**Fabrication of spheroids.** Spheroids were prepared on a silicon dimple plate (DP10-1; Tissue By Net, Tokyo, Japan). NHDFs were collected with TrypLE Express (Thermo Fisher Scientific), and a cell suspension of  $1 \times 10^6$  cells mL<sup>-1</sup> was prepared using FKCM supplemented with 10% FBS and 1% penicillin-streptomycin (Fig. 1A). The cell suspension (20 mL) was seeded in a silicon dimple plate with ~4500 wells (Fig. 1B), and the cells were cultured for 12 h in an incubator at 37°C and 5% CO<sub>2</sub>. Subsequently, spheroids of 200 μm in diameter were formed (Fig. 1C). The spheroids were removed from the dimple plate via pipetting and transferred to a dish as a spheroid suspension. The dish was gently swirled to concentrate the spheroids at the center (Fig. 1D), which were collected using a pipette.

**Creation of cultured dermis.** The net mold was set as 6 mm square in size and 1.0 mm in depth (NM14-2; Tissue By Net) and was used for long-term culture.<sup>22</sup> The diameter and interval of the stainless steel wires were designed to prevent slipping of the spheroids. The prepared spheroids were placed in the frame of a net mold (Fig. 1E) and covered with a net top plate (Fig. 1F). Approximately 40 mL FKCM supplemented with 10% FBS and 1% penicillin-streptomycin was added to a 120-mL sterile container

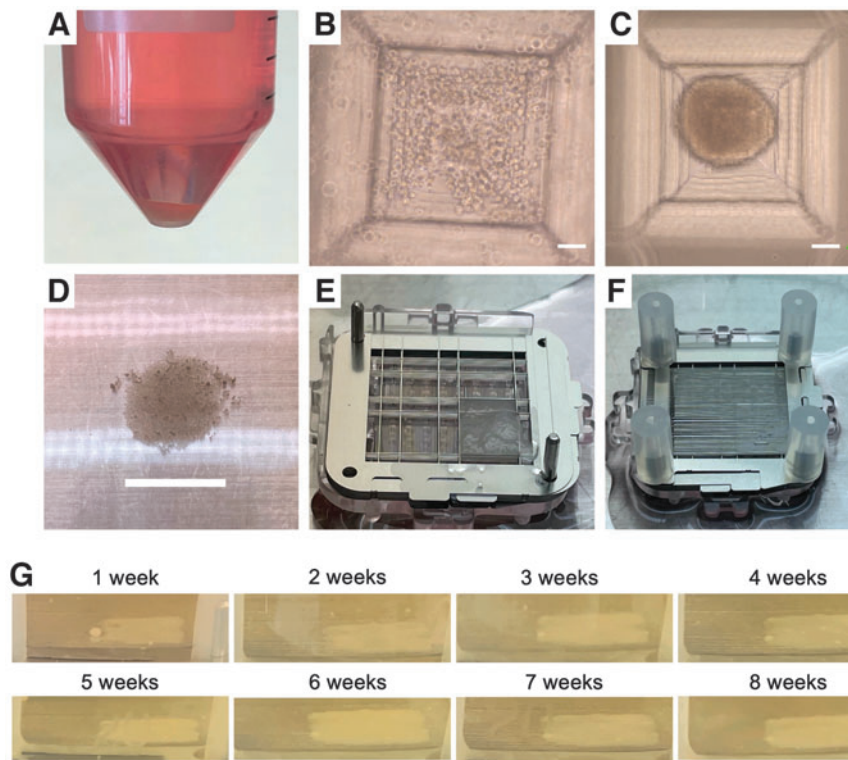


**FIG. 1.** Cell organization process with the net mold. (A) NHDF were collected ( $2 \times 10^7$  cells).

(B) Microscopic observation of the individual well of the silicon dimple plate just after spheroid seeding. Scale bar:  $100 \mu\text{m}$ .

(C) Microscopic observation of the individual well of a silicon dimple plate 12 h after spheroid seeding. Scale bar:  $100 \mu\text{m}$ .

(D) Overall view of the spheroids collected from the dimple plate. Scale bar: 2 cm. (E) The prepared spheroids were filled in the 6 mm frame of the net mold. (F) The spheroids were retained in the net mold by covering with a net top plate.

(G) Weekly progression of the transition from spheroids to cultured dermis over the first 2 months. NHDF, normal human dermal neonatal fibroblasts.

(Thermo Fisher Scientific) and cultured in an incubator at  $37^\circ\text{C}$  and  $5\% \text{CO}_2$  for 2, 4, and 6 months. The containers were placed in a high humidity cell shaker (CS-LR; Taitec, Saitama, Japan) and stirred at 40 rpm to enhance the diffusion of the culture medium.

The cells were cultured for up to 2, 4, and 6 months and half of the medium was changed once a week. During the first 2 months of the experiment, images of the cultured dermis were captured every week while the medium was changed (Fig. 1G).

Following the culture period (2, 4, and 6 months), the cultured dermises were excised from the culture medium and photographed. For *in vitro* analysis, the cultured dermises were excised using punch biopsy tools of 3 mm in diameter (Kai Industries, Gifu, Japan). Tensile strength and dry weight measurements were conducted on 6 mm samples, while all other *in vitro* experiments were conducted using 3 mm samples ( $n=3$  for each group).

#### *In vitro* analysis of cultured dermis

**Histological assessment.** Each sample was fixed with 10% formalin neutral buffer solution (FUJIFILM Wako Pure Chemical Corporation, Osaka, Japan), paraffin embedded, and sectioned at  $5\text{-}\mu\text{m}$  thickness at the center of each specimen. The prepared sections were stained with hematoxylin and eosin (HE), Elastica van Gieson (EVG), and alcian blue. For immunochemical staining, Goat Anti-Type I Collagen-UNLB, Goat Polyclonal Antibody and Goat Anti-Type III Collagen-UNLB, and Goat Polyclonal Antibody (Southern Biotech) were used as the primary antibodies, and Simple Stain Goat MAX-PO (Nichirei Biosciences, Inc., Tokyo, Japan) was used as the secondary antibody. Next, the samples were exposed to 3-3'-diaminobenzidine-4HCl

(DAB; Nichirei Biosciences). The specimens were then observed and photographed with a light microscope (BZ-810; Keyence Corp., Osaka, Japan).

**Tensile strength test.** Each sample was threaded with 5-0 Prolene (Ethicon, Somerville, NJ) in the center, 2.5 mm from its lower edge. The end of the thread was fastened with tape so that the full length of the thread was 5 cm. The samples were set in a tensile strength test apparatus (EZ-LX; Shimadzu, Kyoto, Japan) and the tensile strength test was performed. The maximum value of the test force was determined until breakage at a speed of 100 mm/min. As a control, the strength of collagen-based artificial dermises, Pelnac Gplus<sup>®</sup> (Gunze, Kyoto, Japan) and Integra (Integra Life Sciences Corp., Plainsboro, NJ), were measured in the same way.

**Dry weight measurement.** Each sample was dried for 3 days using a freeze-dryer (VD-250R; Taitec) and the dry weights were measured with an electronic balance (Mettler-Toledo, Greifensee, Switzerland).

**Total collagen assay.** The QuickZyme Total Collagen assay (BioVendor, Brno, Czech Republic) was used to evaluate collagen formation. The collagen assay kit is based on the quantitative colorimetric determination of hydroxyproline residues obtained by the acid hydrolysis of collagen. The absorbance of the reacted reagent was measured at 570 nm using a microplate reader (Varioskan Flash; Thermo Scientific).

**Sulfated glycosaminoglycan assay.** The sGAG content was measured using the Blyscan assay (Biocolor, Carrickfergus, Ireland), following the manufacturer's instructions.

The absorbance of the reacted reagent was measured at 656 nm using the microplate reader (Thermo Scientific).

Evaluation of the cell proliferative capacity of cultured dermis. Each sample was placed in an individual well of a 35 mm tissue culture dish (AGC Techno Glass Co., Ltd., Shizuoka, Japan) and was inverted for 30 min to prevent floating. Approximately 1.5 mL FKCM with 10% FBS was added to each well and incubated at 37°C, 95% humidity, and 5% CO<sub>2</sub>. After 3 and 7 days, migrated fibroblasts were observed using a phase-contrast microscope (ECLIPSE TS100; Nikon, Tokyo, Japan).

The cell proliferative capacity of the cultured dermises was evaluated using the WST-8 (4-[3-(2-methoxy-4-nitrophenyl)-2-[4-nitrophenyl]-2H-5-tetrazolio]-1,3-benzene disulfonate sodium salt) assay (Cell Count Reagent SF; Nacalai Tesque, Co., Ltd., Kyoto, Japan). Each sample was placed into an individual well of a 24-well plate (Thermo Fisher Scientific), and 400 µL FKCM and 40 µL of the test reagent were added to each well and incubated for 2 h at 37°C. Next, three wells of a 96-well plate were each filled with 100 µL of the medium (Thermo Fisher Scientific), and the absorbance of the medium was read using a microplate reader at a test wavelength of 450 nm and a reference wavelength of 650 nm.

#### *In vivo analysis of cultured dermis with a nude-mice full-thickness skin defect model*

**Preparation of cultured dermis.** Cultured dermises were prepared after 4 months of culture ( $n=4$ ). Each cultured dermis was cut into a circular shape of 6 mm in diameter using a punch biopsy tool (Kai Industries). Based on the histological findings, each cultured dermis was divided into two collagen-rich tissues for *in vivo* experiments.

**Experimental design and operative procedure.** Twenty-four BALB/cAJcl-nu/nu mice (male, 7 weeks old) (CLEA Japan, Inc., Tokyo, Japan) were fed and housed individually in a temperature-controlled animal facility with a 12-h light/dark cycle and allocated to three groups: control, cultured dermis, and artificial dermis (Pelnac Gplus). All painful procedures were performed under general anesthesia using isoflurane (Pfizer, Inc., Kyoto, Japan). The concentration of isoflurane was kept at 1.5–2% to provide an appropriate depth of anesthesia. During the application surgery, a donut-shaped silicone skin splint (18/12 mm outer/inner diameter, 0.5 mm in thickness; Fuji System Corp., Tokyo, Japan) was attached to the skin with binding adhesive (Aron Alpha; Daiichi Sankyo, Osaka, Japan). It was then sutured and fixed to the skin using 5-0 nylon (Bear Corporation, Osaka, Japan) to prevent wound contraction.

Next, a full-thickness skin defect, 6 mm in diameter, was made at the center of the applied skin splint using a 6 mm biopsy punch (Kai Industries Co., Ltd., Tokyo, Japan) and scissors. The cultured dermis and artificial dermis were applied to the skin defects in each group, and no sheet was applied in the control group. The wound was covered with a silicone mesh sheet (6 mm in diameter; SI mesh; ALCARE Co., Ltd., Tokyo, Japan) fixed to the marginal skin by suturing with 5-0 nylon, covered with gauze, and secured with a surgical tape bandage (Silkytex, ALCARE Co., Ltd.)

to prevent contamination and mechanical stress. After these procedures were performed, mice were placed in individual cages inside the institutional animal facility.

**Evaluation of wound healing.** The wound-healing process was evaluated on days 7 and 14 postsurgery. Four mice in each group were sacrificed by carbon dioxide gas inhalation at each time point, and macroscopic photographs of the wounds were taken with a digital camera. The wound specimens, including the surrounding tissue, were harvested, fixed in 10% formalin buffer solution (FUJIFILM Wako Pure Chemical Co., Ltd.), paraffin embedded, and sectioned axially at the center of each wound. The specimens were then subjected to HE staining, azocarmine and aniline blue (AZAN) staining, and immunohistochemical staining for CD31.

The neoepithelium length was measured in HE sections on days 7 and 14 postsurgery using an optical microscope (BZ-810; Keyence Corp). The neoepithelium length was defined as the total epithelial length between the innermost hair follicles.

The area of newly formed dermis-like tissue in the wound between the innermost hair follicles and above the muscle layer was measured in AZAN-stained sections using an optical microscope on days 7 and 14. The fibrous connective tissue in granulation was stained light blue with aniline blue, distinguishing it from the dermis of the wound edge, which was stained dark blue. The area of the epidermis that developed over granulation was excluded.

The number and total area of newly formed capillaries were measured on days 7 and 14 in sections immunostained with anti-CD31 antibody. A threshold was set for the brown tint stained with DAB, and the regions with a color density higher than this threshold were counted using the analyzer software (BZ-X800; Keyence Corp.). To measure the capillary area, the area in which the tubular structure of the blood vessels was visible was measured, and the sum of the areas was calculated. Both the capillary number and area were measured in the whole area of newly formed dermis-like tissue, as determined by AZAN staining. However, multiple vessel cross sections observed on a two-dimensional section may originate from a single vessel; therefore, the number and areas of capillaries per unit granulation area observed in the sections were evaluated according to the method used in previous studies.<sup>23,24</sup>

#### *Statistical analysis*

Statistical significance was assessed using the Tukey–Kramer multiple comparisons test. All data are expressed as mean ± standard deviation. Statistical significance was set at  $p < 0.05$ .

## **Results**

### *Gross appearance of cultured dermis*

The sequential photographs in Figure 1G indicate the absence of significant visible changes in the appearance of the cultured dermis. As illustrated in Figure 2A, cultured dermises were produced using net-mold cultures at each time point, and the surface of the tissues appeared shiny and flat on both the top and bottom.

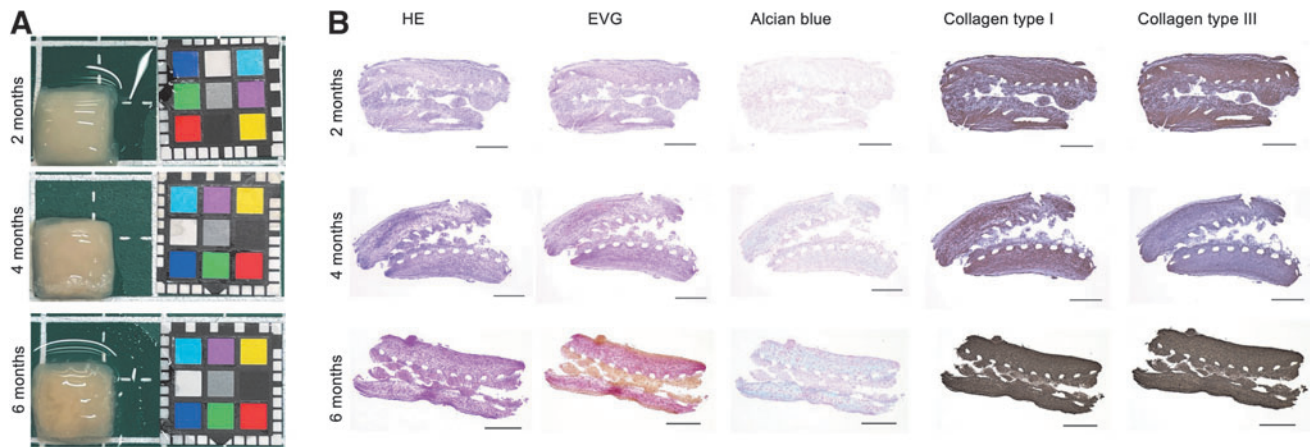


**FIG. 2.** Gross appearance and histological evaluation of the cultured dermis. **(A)** The cultured dermis was generated via a long-term culture with the net-mold. Photographs of the cultured dermises at 2, 4, and 6 months, respectively, are shown. Color scale: 10 mm. **(B)** The prepared sections were stained with HE, EVG, and alcian blue, and underwent immunochemical staining (collagen type I and collagen type III). Scale bar: 500  $\mu$ m. EVG, elastic van Gieson; HE, hematoxylin and eosin.

*In vitro analysis of cultured dermis*

**Histological assessment of cultured dermis.** At all time points, the internal part of the cultured dermis was fragile and two collagen-rich tissues were formed toward the outside of the net mold (Fig. 2B). According to EVG staining, the cultured dermis was predominantly composed of collagen fibers. Alcian blue staining revealed that acidic mucopolysaccharides were mainly present in the intermediate layer of the cultured dermis. Immunostaining with anti-type I or anti-type III collagen antibodies indicated that type I and III collagen were widely distributed throughout the cultured dermis.

**Tensile strength analysis.** The average tensile strength of the dermises cultured for 4 and 6 months was significantly higher than that of the dermis cultured for 2 months ( $n=3$ ) (Fig. 3A). As a control, the strength of the collagen-based artificial dermis, Pelnac Gplus and Integra, was

$0.063 \pm 0.014$  and  $0.15 \pm 0.018$  N, respectively. The average tensile strength of the dermis cultured for 4 months was significantly higher than that of the artificial dermis (Fig. 3B).

Dry weight, total collagen, sGAG, and cell proliferative capacity analysis of cultured dermis. The average dry weights of the dermises cultured for 2, 4, and 6 months were not significantly different (Fig. 4A). The total collagen of the dermis cultured for 2 months was significantly higher than that of the dermises cultured for 4 and 6 months (Fig. 4B). The average sGAG content of the dermis cultured for 2 months was significantly higher than that of the dermis cultured for 6 months (Fig. 4C).

Figure 5A displays the outgrowth fibroblasts after 3 and 7 days of cultivation. The average absorbance (450–650 nm) of the dermises cultured for 2, 4, and 6 months were not significantly different (Fig. 5B).

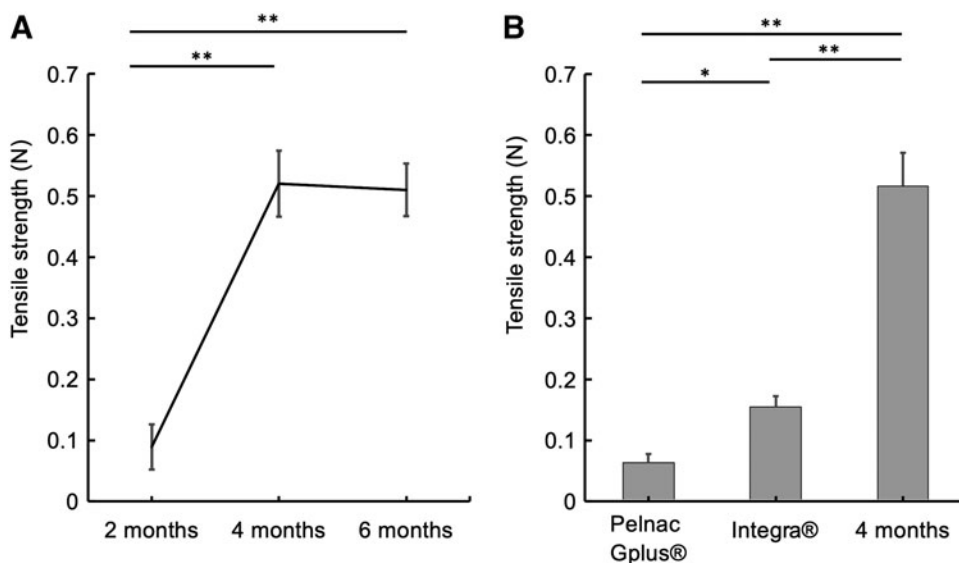


**FIG. 3.** Tensile strength test. **(A)** Analysis of the tensile strength of the cultured dermis.  $n=3$ . Error bars: SD.  $**p < 0.01$  represents significance between groups. **(B)** Analysis of the tensile strength of the 4 month-cultured dermis compared with that of the artificial dermis (Pelnac Gplus® and Integra®).  $n=3$ . Error bars: SD.  $*p < 0.05$  and  $**p < 0.01$ , respectively, represent significance between groups. SD, standard deviation.

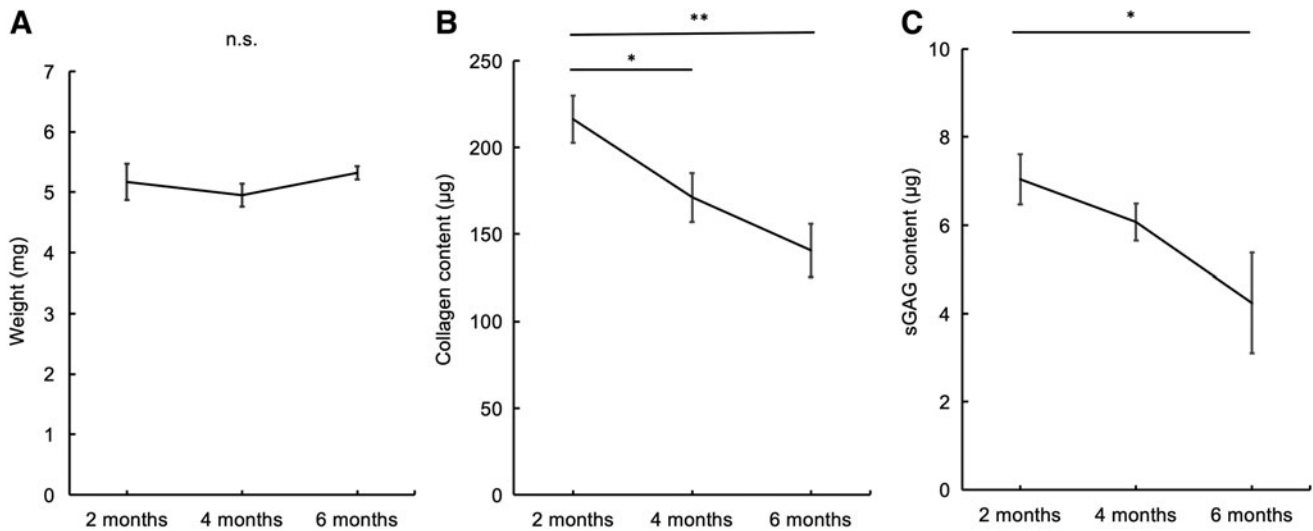


**FIG. 4.** Quantitative analysis of the cultured dermis. **(A)** Analysis of the dry weight of the 6 mm square cultured dermis generated by long-term culture; 2, 4, and 6 months.  $n=3$ . Error bars: SD. There was no significant difference between the groups. **(B)** Analysis of the collagen content of the 3 mm diameter cultured dermis.  $n=3$ . Error bars: SD.  $*p<0.05$  and  $**p<0.01$  respectively, represent significance between groups. **(C)** Analysis of the sGAG content of the 3 mm diameter cultured dermis.  $n=3$ . Error bars: SD.  $*p<0.05$  represent significance between groups. sGAG, sulfated glycosaminoglycans.

#### In vivo analysis of cultured dermis with a nude-mice full-thickness skin defect model

On days 7 and 14 postsurgery, the wounds were covered with crusts. No obvious signs of infection were noted at any time (Fig. 6). The neoepithelium length in the cultured dermis group was significantly longer than that in the control group on day 14 (Fig. 7). In AZAN-stained sections, the average areas of newly formed dermis-like tissue in each group were not significantly different (Fig. 8). The area of new capillaries in the cultured dermis group was significantly larger than those in the control group and artificial dermis group; however, the number of capillaries in each group was not significantly different (Fig. 9).

#### Discussion

This report presents the first successful development of a self-assembled, cell-based dermal substitute derived from human dermal fibroblasts through long-term 3D culture. Spheroids were generated from fibroblasts as a preliminary step to meet the size requirement ( $\sim 200 \mu\text{m}$ ) imposed by the net-mold, which consists of stainless-steel wires combined at  $100 \mu\text{m}$  intervals, to prevent any leakage. The culture medium FKCM, which contains  $10 \text{ ng mL}^{-1}$  of epidermal growth factor, was reported to be suitable for fibroblast culture as it enhances ECM production, cell migration, and cell proliferation.<sup>25,26</sup> The dry weight and cell proliferative capacity of the cultured dermis did not decrease over

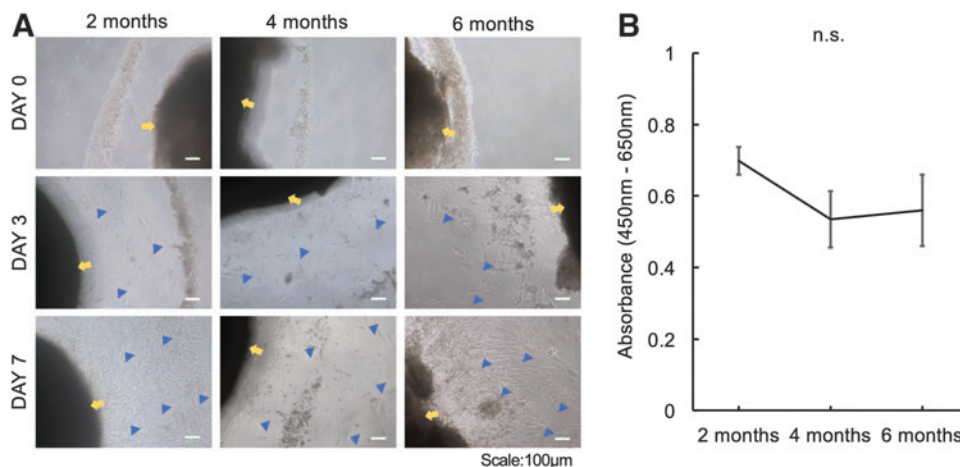


**FIG. 5.** Evaluation of the cell proliferative capacity of the cultured dermis. Absorbance of the medium 2 h after the incubation of the 3 mm diameter cultured dermis generated by long-term culture; 2, 4, and 6 months.  $n=3$ . **(A)** Micrographs of the outgrowth of fibroblasts on day 0, 3, and 7. Yellow arrows indicate the cultured dermis and blue arrowheads indicate fibroblast outgrowth. Scale bar:  $100 \mu\text{m}$ . **(B)** The cell proliferative capacity of the cultured dermis was evaluated using the WST-8 assay. The absorbance of the medium was analyzed using a microplate reader at a test wavelength of 450 nm and a reference wavelength of 650 nm. There was no significant difference between the groups. WST-8, 4-[3-(2-methoxy-4-nitrophenyl)-2-[4-nitrophenyl]-2H-5-tetrazolio]-1,3-benzene disulfonate sodium salt.

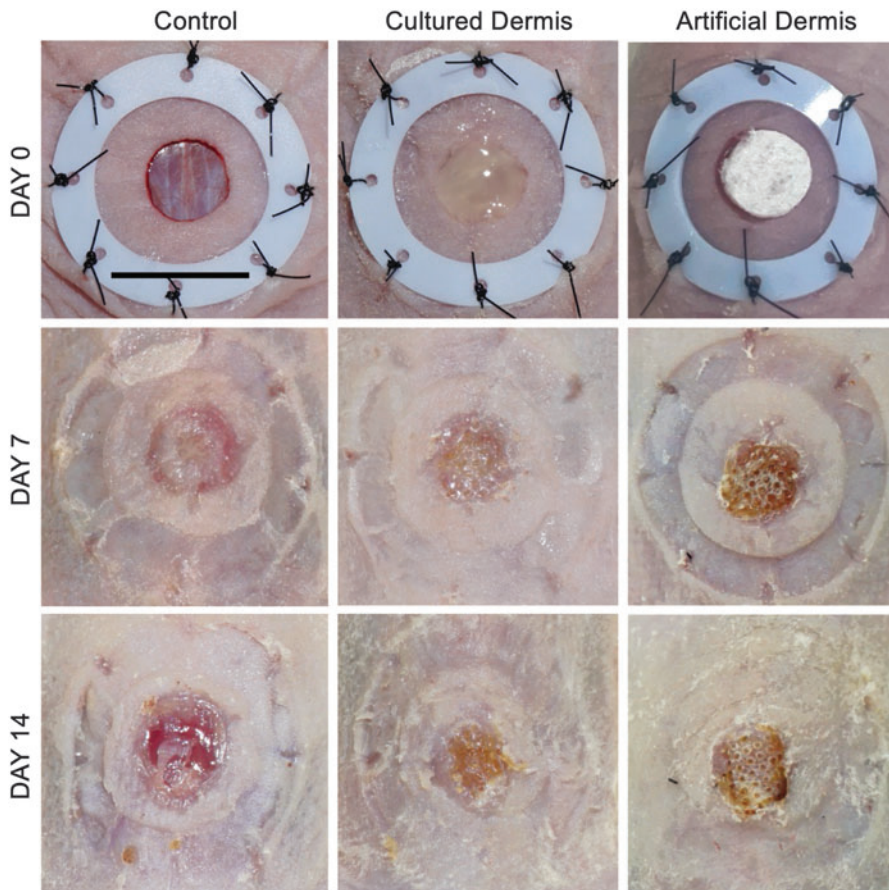


**FIG. 6.** Macroscopic photographs of the wounds. Wound area in the control, cultured dermis, and artificial dermis groups on the day of surgery, and on days 7 and 14 postsurgery. Scale bar: 1 cm.

time, suggesting that the fibroblasts were the main components of the cultured dermis and that the cell quantity remained relatively stable.

Although the amount of collagen and sGAG in the cultured dermis decreased over time, the tensile strength of the cultured dermis increased significantly after 4 months of culture, suggesting that remodeling had occurred, leading to the formation of a more robust network.<sup>27</sup> In addition, fibroblasts in the cultured dermis were still able to proliferate and grow after 6 months of culture, unlike those in culture dishes. ECM composition and organization play a crucial role in numerous biological processes ranging from cell migration, differentiation, and survival.<sup>28,29</sup>

Sakaguchi et al. demonstrated that increasing the thickness of 3D tissue resulted in the death of cells inside the tissue; however, tissue with a thickness of 1.2 mm or less did not exhibit internal defects, even after 3 weeks of culture. They concluded that the diffusion limit was  $\sim 600 \mu\text{m}$  from the surface of the 3D tissue.<sup>22</sup> In this study, the thickness of the net mold was set to 1.0 mm to maintain cell viability during long-term culture. However, the inner part of the cultured dermis became fragile over the 2 months of culture, leading to the formation of two 3D tissues with a thickness of  $400 \mu\text{m}$  each. This was likely due to the loss of tissue porosity during ECM remodeling, which impeded the diffusion of liquid components.

The two tissues obtained by dividing the 4-month cultured dermis had a thickness equivalent to that of human split-thickness skin grafts and had sufficient strength to be sutured. In *in vivo* experiments, this self-assembled cultured

dermis significantly promoted angiogenesis and neopithelialization compared to the collagen-based artificial dermis. This favorable result can be attributed to the properties of fibroblasts. Wound healing in the skin defect model depends on the coordinated collective activity of several cell types, with dermal fibroblasts known to play a pivotal role in mediating fibrosis, participating in inflammatory networks, synthesizing matrix, and modulating immune cell functions.<sup>6</sup> In addition, fibroblasts have the potential to contribute to angiogenesis during wound healing.<sup>30</sup>

Although significant difference in neovascularization was not observed between the cultured dermis and the other groups at 7 days posttransplantation, intriguingly, the cultured dermis group exhibited the sustained presence of induced new capillaries even after 14 days. These findings suggest the existence of a distinct neovascularization process in the cultured dermis group compared to that in the other groups. The efficient and timely induction of a new vascular supply is considered a critical factor for graft survival.<sup>31</sup>

Our findings suggest the superiority of the scaffold-free cultured dermis in terms of sufficient tensile strength, high biocompatibility, and efficacy in promoting wound healing. Such self-assembled, cell-based dermal substitutes are highly promising for permanent skin coverage when combined with cultured keratinocyte sheets. However, there is a need for further improvement, such as shortening of the culture period and increasing the size of the cultured dermis. In particular, methods such as application of physical stimulation (e.g., stretching, compression, or electrical stimulation) to the cultured dermis using a bioreactor can be

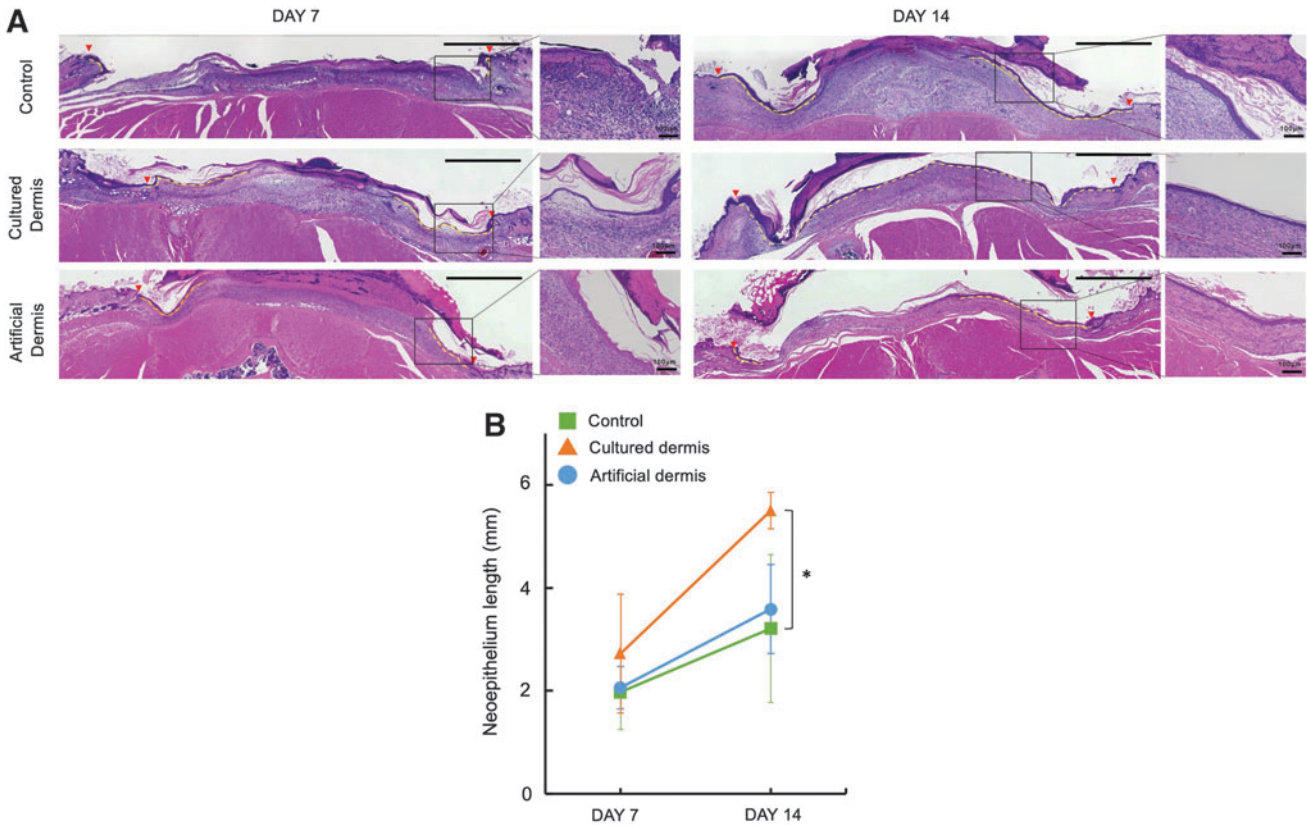


**FIG. 7.** Neopithelium length on days 7 and 14 postsurgery. **(A)** The HE-stained sections of the wounds in the control, cultured dermis, and artificial dermis groups. The *yellow dashed line* indicates the newly formed epithelium. Scale bar: 1 mm. **(B)** Length of the epithelium in the wounds of the control, cultured dermis, and artificial dermis groups. The epithelial length of the cultured dermis groups was significantly higher than that of the control group on days 14. (\* $p < 0.05$ ,  $n = 4$ ). Error bars show SD.

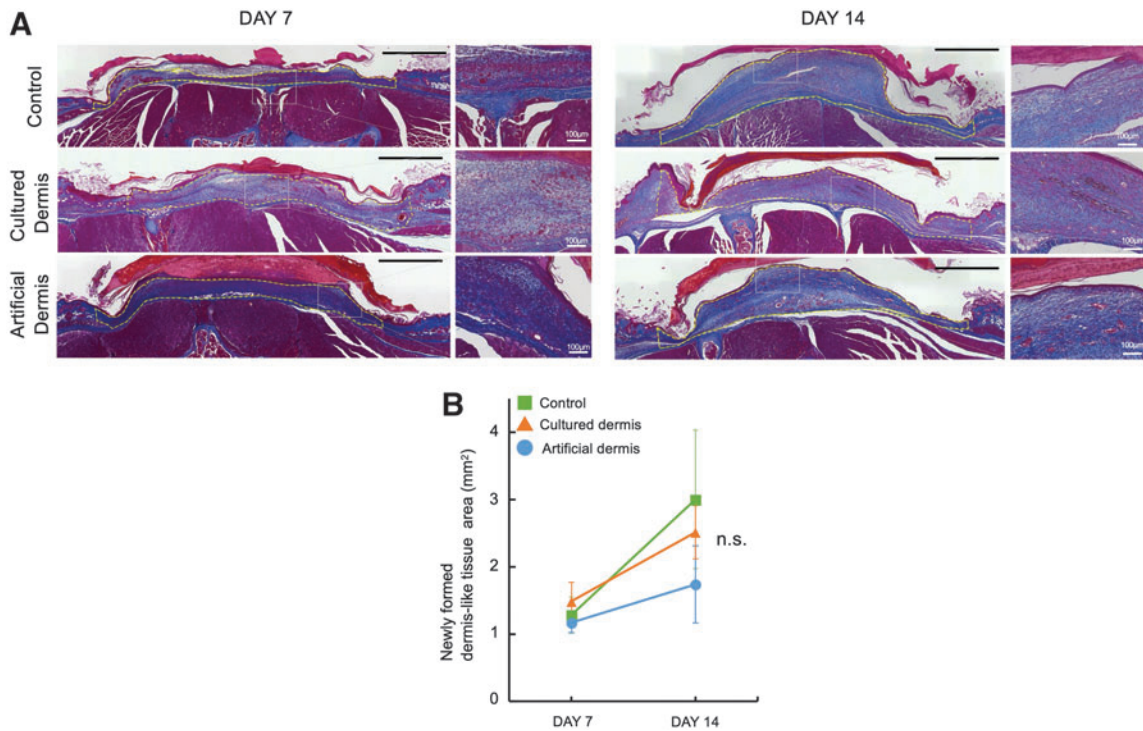


**FIG. 8.** Newly formed dermis-like tissue area on days 7 and 14 postsurgery. **(A)** The AZAN-stained sections of the wounds in the control, cultured dermis, and artificial dermis groups. The *yellow dashed line* indicates the newly formed dermis-like tissue area. Scale bar: 1 mm. **(B)** The newly formed dermis-like tissue area in the wounds of the control, cultured dermis, and artificial dermis groups. Significant differences between the groups were not observed on days 7 or 14. ( $n = 4$ ). Error bars show SD. AZAN, azocarmine and aniline blue.

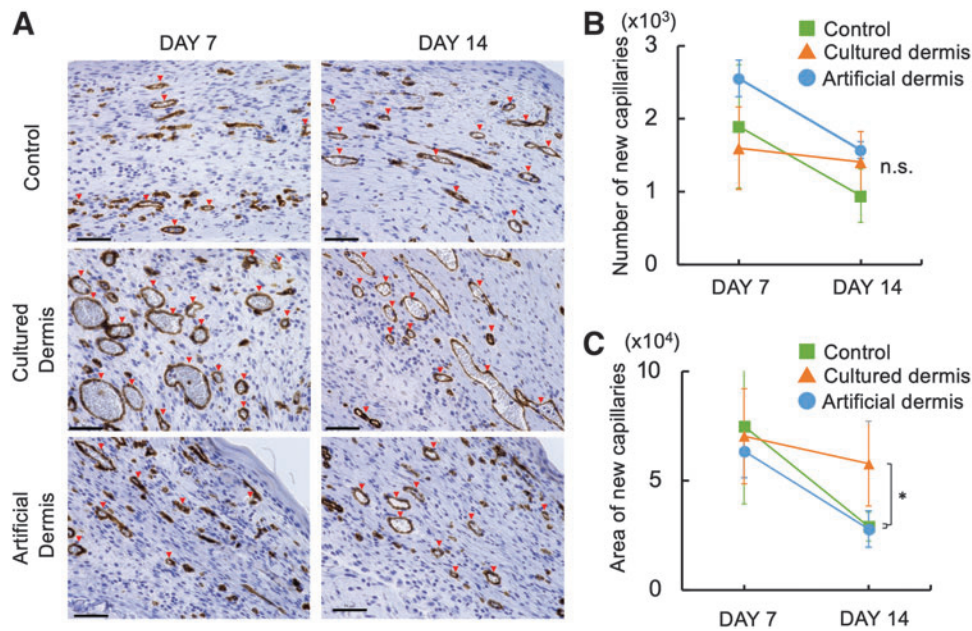


**FIG. 9.** Newly formed capillaries on days 7 and 14 postsurgery. **(A)** The sections immunostained with anti-CD31 antibody in the control, cultured dermis, and artificial groups. The red arrowheads (*filled triangle*) indicate the newly formed capillaries. Scale bar: 50  $\mu\text{m}$ . **(B)** The number of newly formed capillaries on days 7 and 14. Significant differences between the groups were not observed on days 7 or 14. ( $n=4$ ). Error bars show SD. **(C)** The total area of newly formed capillaries in the cultured dermis group was significantly larger than those of the control group and artificial dermis group on day 14. ( $*p<0.05$ ,  $n=4$ ). Error bars show SD.

considered as possible approaches.<sup>32</sup> In addition, to better mimic the native dermis, an approach that combines multiple cell types that constitute the dermis, including appendages such as hair follicles and eccrine glands, could be considered.

This study has some limitations. First, the sample size of the experiment was limited due to the restriction on the number of samples that could be generated. Second, *in vitro* tensile strength measurements were only conducted on the predivided cultured dermis, whereas *in vivo* experiments were performed using divided tissues. Third, the possibility of differences between the two divided tissues was not taken into consideration. Owing to the different directions of gravity and the slight variations in depth from the liquid surface of the culture medium, the size and other characteristics may differ between the upper and lower parts of the cultured dermis.

## Conclusions

To the best of our knowledge, this is the first report of the successful development of a self-assembled, cell-based dermal substitute derived from human dermal fibroblasts through long-term 3D culture. The scaffold-free cultured dermis exhibited superior properties, such as sufficient tensile strength, high biocompatibility, and efficacy in promoting wound healing, when compared to the collagen-based artificial dermis. Although further studies are needed, we believe that the cultured dermis has the potential to be an innovative material for permanent skin coverage.

## Acknowledgments

The authors thank Rie Tatsumi and Yasuko Minaki for their generous assistance, and Editage (www.editage.com) for English language editing.

## Authors' Contributions

T.N. collected, analyzed, and interpreted the data and drafted the article. H.Y. contributed to data interpretation, drafted the article, and critically revised the article. M.S. collected and analyzed the data and drafted the article. I.T. and Y.K. collected, analyzed, and interpreted the data. S.S. interpreted data and critically revised the article. J.O. and T.Y. conceived the ideas and drafted the article. N.M. conceived the ideas, designed and approved the study, collected and interpreted the data, and critically revised the article. All authors gave final approval and agree to be accountable for all aspects of the work.

## Author Disclosure Statement

No competing financial interests exist.

## Funding Information

This research was supported by the Translational Research Network Program (Seeds A) of the Japanese Agency for Medical Research and Development (AMED) under grant number 22ym0126808j0001-A-193.

## References

- Sorg H, Tilkorn DJ, Hager S, et al. Skin wound healing: An update on the current knowledge and concepts. *Eur Surg Res Eur* 2017;58(1–2):81–94; doi: 10.1159/000454919
- Shahrokhi S, Arno A, Jeschke MG. The use of dermal substitutes in burn surgery: Acute phase. *Wound Repair Regen* 2014;22(1):14–22; doi: 10.1111/wrr.12119
- Dai C, Shih S, Khachemoune A. Skin substitutes for acute and chronic wound healing: An updated review.

- J Dermatol Treat 2020;31(6):639–648; doi: 10.1080/09546634.2018.1530443
4. Atiyeh BS, Costagliola M. Cultured epithelial autograft (CEA) in burn treatment: Three decades later. *Burns* 2007;33(4):405–413; doi: 10.1016/j.burns.2006.11.002
  5. Egaña JT, Danner S, Kremer M, et al. The use of glandular-derived stem cells to improve vascularization in scaffold-mediated dermal regeneration. *Biomaterials* 2009;30(30):5918–5926; doi: 10.1016/j.biomaterials.2009.07.023
  6. Rippa AL, Kalabusheva EP, Vorotelyak EA. Regeneration of dermis: Scarring and cells involved. *Cell* 2019;18;8(6):607.
  7. Sriram G, Bigliardi PL, Bigliardi-Qi M. Fibroblast heterogeneity and its implications for engineering organotypic skin models in vitro. *Eur J Cell Biol* 2015;94(11):483–512; doi: 10.1016/j.ejcb.2015.08.001
  8. Vig K, Chaudhari A, Tripathi S, et al. Advances in skin regeneration using tissue engineering. *Int J Mol Sci* 2017;18(4); doi: 10.3390/ijms18040789
  9. Halim AS, Khoo TL, Mohd Yusoff SJ. Biologic and synthetic skin substitutes: An overview. *Indian J Plast Surg* 2010;43(Suppl):S23–S28; doi: 10.4103/0970-0358.70712
  10. Harrison CA, Gossiel F, Layton CM, et al. Use of an in vitro model of tissue-engineered skin to investigate the mechanism of skin graft contraction. *Tissue Eng* 2006;12(11):3119–3133; doi: 10.1089/ten.2006.12.3119
  11. Egaña JT, Fierro FA, Krüger S, et al. Use of human mesenchymal cells to improve vascularization in a mouse model for scaffold-based dermal regeneration. *Tissue Eng Part A* 2009;15(5):1191–1200; doi: 10.1089/ten.tea.2008.0097
  12. Liu S, Zhang H, Zhang X, et al. Synergistic angiogenesis promoting effects of extracellular matrix scaffolds and adipose-derived stem cells during wound repair. *Tissue Eng Part A* 2011;17(5–6):725–739; doi: 10.1089/ten.TEA.2010.0331
  13. Bell E, Ivarsson B, Merrill C. Production of a tissue-like structure by contraction of collagen lattices by human fibroblasts of different proliferative potential in vitro. *Proc Natl Acad Sci U S A* 1979;76(3):1274–1278; doi: 10.1073/pnas.76.3.1274
  14. Tomasek JJ, Haaksma CJ, Eddy RJ, et al. Fibroblast contraction occurs on release of tension in attached collagen lattices: Dependency on an organized actin cytoskeleton and serum. *Anat Rec* 1992;232(3):359–368; doi: 10.1002/ar.1092320305
  15. Rnjak J, Wise SG, Mithieux SM, et al. Severe burn injuries and the role of elastin in the design of dermal substitutes. *Tissue Eng Part B Rev* 2011;17(2):81–91; doi: 10.1089/ten.TEB.2010.0452
  16. Matsumura H, Matsushima A, Ueyama M, et al. Application of the cultured epidermal autograft “JACE<sup>®</sup>” for treatment of severe burns: Results of a 6-year multicenter surveillance in Japan. *Burns* 2016;42(4):769–776; doi: 10.1016/j.burns.2016.01.019
  17. Klingenberg JM, Mcfarland KL, Friedman AJ, et al. Engineered human skin substitutes undergo large-scale genomic reprogramming and normal skin-like maturation after transplantation to Athymic Mice. *J Invest Dermatol* 2010;130(2):587–601; doi: 10.1038/jid.2009.295
  18. Sander EA, Boyce ST. Development of the mechanical properties of engineered skin substitutes after grafting to full-thickness wounds. 2014;136(May):1–7; doi: 10.1115/1.4026290
  19. Nicholas MN, Jeschke MG, Amini-Nik S. Methodologies in creating skin substitutes. *Cell Mol Life Sci* 2016;73(18):3453–3472; doi: 10.1007/s00018-016-2252-8
  20. Klimov M, Medeiros E, Farkash EA, et al. Bioengineered Self-assembled skin as an alternative to skin grafts. *Plast Reconstr Surg Glob Open* 2016;4(6):e731; doi: 10.1097/GOX.0000000000000723
  21. Wilks BT, Evans EB, Nakhla MN, et al. Directing fibroblast self-assembly to fabricate highly-aligned, collagen-rich matrices. *Acta Biomater* 2018;81:70–79; doi: 10.1016/j.actbio.2018.09.030
  22. Sakaguchi K, Tobe Y, Yang J, et al. Bioengineering of a scaffold-less three-dimensional tissue using net mould. *Biofabrication* 2021;13(4); doi: 10.1088/1758-5090/ac23e3
  23. Kanda N, Morimoto N, Takemoto S, et al. Efficacy of novel collagen/gelatin scaffold with sustained release of basic fibroblast growth factor for dermis-like tissue regeneration. *Ann Plast Surg* 2012;69(5):569–574; doi: 10.1097/SAP.0b013e318222832f
  24. Sakamoto M, Morimoto N, Ogino S, et al. Efficacy of gelatin gel sheets in sustaining the release of basic fibroblast growth factor for murine skin defects. *J Surg Res* 2016;201(2):378–387; doi: 10.1016/j.jss.2015.11.045
  25. Busco G, Cardone RA, Greco MR, et al. NHE1 promotes invadopodial ECM proteolysis through acidification of the peri-invadopodial space. *FASEB J* 2010;24(10):3903–3915; doi: 10.1096/fj.09-149518
  26. Kokai Y, Myers JN, Wada T, et al. Synergistic interaction of p185c-neu and the EGF receptor leads to transformation of rodent fibroblasts. *Cell* 1989;58(2):287–292; doi: 10.1016/0092-8674(89)90843-x
  27. Chen K, Henn D, Januszzyk M, et al. Disrupting mechanotransduction decreases fibrosis and contracture in split-thickness skin grafting. *Sci Transl Med* 2022;14(645):eabj9152; doi: 10.1126/scitranslmed.abj9152
  28. Walker C, Mojares E, Del Río Hernández A. Role of extracellular matrix in development and cancer progression. *Int J Mol Sci* 2018;19(10); doi: 10.3390/ijms19103028
  29. Mouw JK, Ou G, Weaver VM. Extracellular matrix assembly: A multiscale deconstruction. *Nat Rev Mol Cell Biol* 2014;15(12):771–785; doi: 10.1038/nrm3902
  30. Shamis Y, Silva EA, Hewitt KJ, et al. Fibroblasts derived from human pluripotent stem cells activate angiogenic responses in vitro and in vivo. *PLoS One* 2013;8(12):e83755; doi: 10.1371/journal.pone.0083755
  31. Tremblay P-L, Hudon V, Berthod F, et al. Inoculation of tissue-engineered capillaries with the host’s vasculature in a reconstructed skin transplanted on mice. *Am J Transplant* 2005;5(5):1002–1010; doi: 10.1111/j.1600-6143.2005.00790.x
  32. Ravichandran A, Liu Y, Teoh SH. Review: Bioreactor design towards generation of relevant engineered tissues: Focus on clinical translation. *J Tissue Eng Regen Med* 2018;12(1):e7–e22; doi: 10.1002/term.2270

Address correspondence to  
Hiroki Yamanaka, MD, PhD

Department of Plastic and Reconstructive Surgery  
Graduate School of Medicine  
Kyoto University  
54 Shogoin-Kawahara-cho  
Kyoto 606-8507  
Japan

E-mail: ymnkahrk@kuhp.kyoto-u.ac.jp

Received: May 15, 2023

Accepted: July 27, 2023

Online Publication Date: September 14, 2023